Journal of Power Sources 195 (2010) 8080–8083

Contents lists available at ScienceDirect

Journal of Power Sources

journal homepage: www.elsevier.com/locate/jpowsour

Short communication

Nitrogen-doped multi-walled carbon nanocoils as catalyst support for oxygen reduction reaction in proton exchange membrane fuel cell

R. Imran Jafri [a], N. Rajalakshmi [b], S. Ramaprabhu [a,*]

[a] Alternative Energy and Nanotechnology Laboratory (AENL), Nano Functional Materials Technology Centre (NFMTC), Department of Physics, Indian Institute of Technology Madras, Chennai, India
[b] Centre for Fuel cell Technology, IIT Madras Research Park, 6, Kanagam Road, Taramani, Chennai 600 113, India

ARTICLE INFO

Article history:
Received 25 March 2010
Received in revised form 20 June 2010
Accepted 23 June 2010
Available online 13 July 2010

Keywords:
Carbon nanocoils
Nitrogen doping
Electrocatalyst
Proton-exchange membrane fuel cell
Polarization graphs

ABSTRACT

Multi-walled carbon nanocoils (MWNCs) are synthesized by chemical vapour deposition and nitrogen-doped MWNCs (N-MWNCs) are obtained by nitrogen plasma treatment. MWNCs and N-MWNCs are used as catalyst supports for platinum nanoparticles. Pt nanoparticles are dispersed over these support materials using the conventional chemical reduction technique and then used for the oxygen reduction reaction in proton-exchange membrane fuel cells. The morphology and structure of the MWNC-based powder samples are studied by means of scanning electron microscopy, transmission electron microscopy, X-ray diffraction, and Raman spectroscopy. Full cells are constructed with Pt-loaded MWNC/N-MWNC and the results are discussed. A maximum power density of 550 and 490 mW cm^{-2} is obtained with Pt/N-MWNC and Pt/MWNC as the ORR catalyst, respectively. The improved performance of a fuel cell with a N-MWNC catalyst support can be attributed to the creation of pyrrolic nitrogen defects due to the nitrogen plasma treatment. These defects act as good anchoring sites for the deposition of Pt nanoparticles and to the increased electrical conductivity and improved carbon-catalyst binding.

1. Introduction

In proton-exchange membrane fuel cells (PEMFCs), Pt-based electrocatalysts are widely used as anode and cathode electrocatalysts for the hydrogen oxidation and the oxygen reduction reactions, respectively. One-dimensional carbon nanotubes (CNTs), with their high surface area and nanosize morphology, possess several unique features such as the ability to carry large current densities and fast electron transfer kinetics when used as electrodes for electrochemical sensing and supercapacitor applications [1–3]. One promising application of CNTs is to act as a support for metal catalysts (Pt) on account of their large surface area, good conductivity, and high chemical stability [4–6]. Another type of interesting carbon nanostructure are carbon nanocoils (CNCs) which can be synthesized by the creation of pentagon and heptagon defects at regular intervals during the growth of CNTs. The CNCs exhibit some interesting mechanical and electromagnetic properties due to their peculiar helical morphologies, in addition to the excellent properties of CNTs. Hayashida et al. [7] have reported a conductivity of 100–180 S cm^{-1} and a Young modulus of 0.1 TPa for CNCs which is slightly smaller than that for straight CNTs [8]. Chen et al. [9] also reported that a CNC behaves as an elastic spring with a spring constant K of 0.12 N m^{-1} in the low-strain regime, with an upturn in K in the high-stain regime. These excellent electrical properties and helical shapes make CNCs potential candidates for fuel cell applications [10,11].

The purpose of the carbon support is to stabilize the Pt nanoparticles and increasing this interaction helps to improve the durability of the catalyst by resisting any changes that would limit its efficiency. It has been widely reported that nitrogen-doped carbon nanostructures show *n*-type or metallic behaviour and are expected to have greater electron mobility than the corresponding un-doped carbon nanostructures. Moreover, nitrogen doping efficiently introduces chemically active sites for use in catalytic reactions and also acts as anchoring sites for metal nanoparticle deposition. It has been demonstrated [12–16] that nitrogen-doped carbon supports can increase the durability and activity of a Pt catalyst. Different techniques have been employed for the synthesis of nitrogen-doped nanostructures; these can be broadly classified into in situ doping, postdoping [17–21] and plasma treatment [22]. The present work demonstrates the improvement in the performance of a PEMFC when nitrogen-doped multi-walled carbon nanocoils (N-MWNCs) prepared by plasma treatment of multi-walled carbon nanocoils (MWNCs) are employed as a catalyst support material for the oxygen reduction reaction (ORR).

* Corresponding author. Tel.: +91 44 22574862; fax: +91 44 22574852.
E-mail address: ramp@iitm.ac.in (S. Ramaprabhu).

0378-7753/$ – see front matter © 2010 Elsevier B.V. All rights reserved.
doi:10.1016/j.jpowsour.2010.06.109

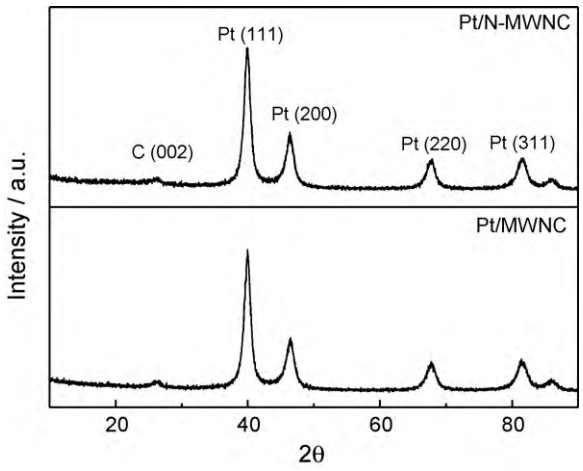

Fig. 1. XRD pattern of Pt/MWNCs and Pt/N-MWNCs.

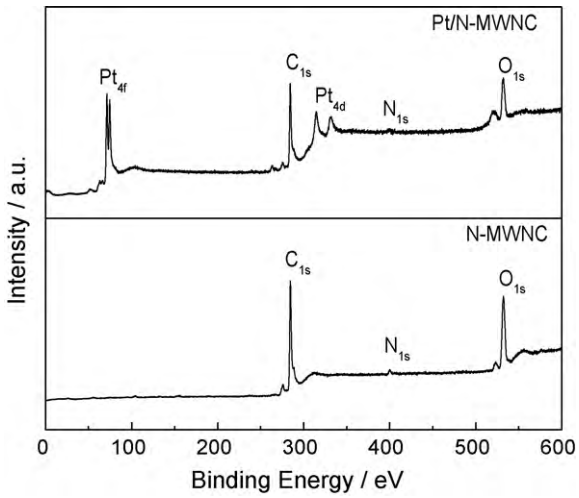

Fig. 3. XPS survey spectra of N-MWNCs and Pt/N-MWNCs.

2. Experimental

Multi-walled carbon nanocoils were prepared by pyrolysis of acetylene over $MmNi_3$-coated carbon cloth in a chemical vapour deposition (CVD) unit. $MmNi_3$ was coated over carbon cloth using an RF sputter deposition technique and was hydrogen decrepitated (hydrogenation and de-hydrogenation) several time before loading into the CVD unit [23]. The as-grown MWNCs were purified and funtionalized following the procedure mentioned in earlier work [33]. Multi-walled carbon nanotubes (MWNTs) prepared by the pyrolysis of acetylene over AB_3-based alloy hydride catalyst [33] has also been functionalized following a similar process. Nitrogen plasma treatment of the MWNCs was performed in a planar RF magnetron sputtering system (Hind High Vac Pvt. Ltd., Bengaluru, India) equipped with a high frequency generator operating at 13.56 MHz and a power up to 500 W. About 200 mg of MWNCs were placed on a glass plate and introduced into the plasma chamber for 30 min; the chamber pressure and plasma power were maintained at 0.1 mbar and 130 W, respectively.

Platinum-loaded MWNTs (Pt/MWNTs), platinum-loaded MWNCs (Pt/MWNCs) and platinum-loaded N-MWNCs (Pt/N-MWNCs) were prepared by a chemical reduction technique [33]. Briefly, 1 g of support material (MWNTs, MWNCs and N-MWNCs) was ultra sonicated in 50 ml of de-ionized water for 1 h followed by stirring magnetically for 4 h. The required amount of 1% solution of hexachloroplatinic acid was added to obtain a 40 wt.% Pt loading. The Pt salt was reduced by slowly adding a solution of 0.1 M $NaBH_4$ in 1 M NaOH. After completion of the reaction, the solution was washed, filtered and dried at 80 °C for 3 h. The samples were characterized by means of X-ray diffraction (XRD; Philips X'pert Pro X-ray diffractometer with Cu K_α radiation of 1.541 å), Raman spectroscopy (Horiba Jobin Yvon HR800), transmission electron microscopy (TEM; Philips JEOL CM12), and X-ray photoelectron spectroscopy (XPS; Omicron Nanotechnology).

Fuel cell measurements were performed with an ElectroChem Fuel Cell Test Station. A membrane electrode assembly (MEA) was prepared by sandwiching a pretreated Nafion 212 CS® membrane between the anode and the cathode. Pretreatment of the Nafion membrane was performed by boiling in a solution of 5% H_2O_2 and 1 M H_2SO_4, successively, at 80 °C for 30 min and washing several times with de-ionized water after each step. Both the anode and the cathode were comprised of a backing layer, a gas-diffusion layer, and a catalyst layer. The catalyst layer was prepared by ultrasonicating the required amount of catalyst in de-ionized water. Typically, 0.3 ml of 5 wt.% Nafion was added to 15 mg of electrocatalyst (Pt/MWNTs) on the anode side and 0.6 ml of 5 wt.% Nafion was added to 30 mg of electrocatalyst (Pt/N-MWNCs) on the cathode side, thus maintaining a fixed Nafion to electrocatalyst ratio of 1:1 (by weight). The suspension was coated uniformly over gas-

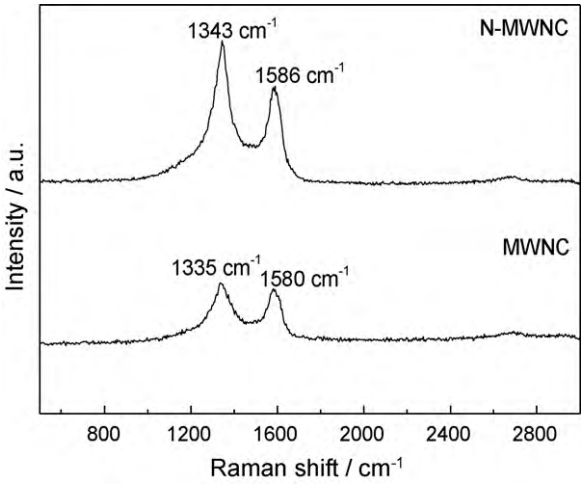

Fig. 2. Raman spectrum of MWNCs and N-MWNCs.

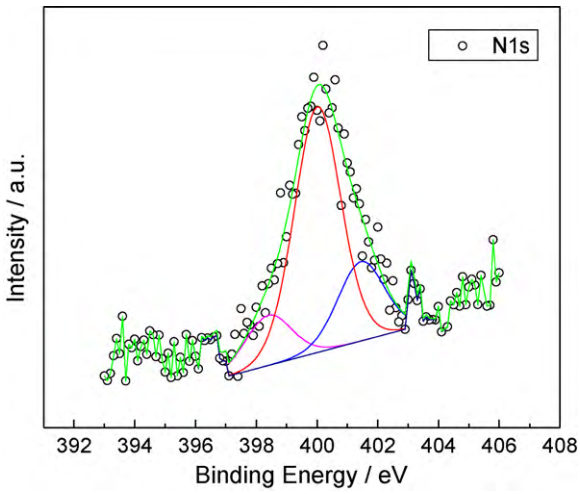

Fig. 4. The de-convoluted N1s region.

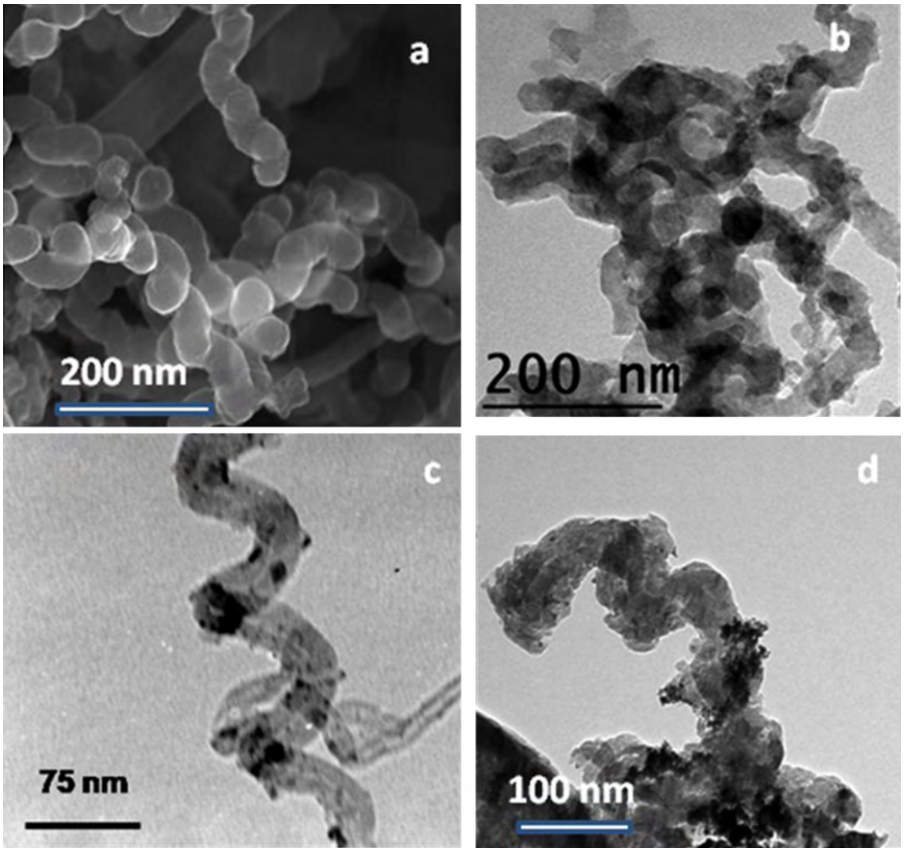

Fig. 5. SEM image of (a) MWNCs, TEM images of (b) N-MWNCs, (c) Pt/MWNCs and (d) Pt/N-MWNCs.

diffusion layer. A mixture of carbon (Vulcan XC 72) and polytetra flouro ethylene (PTFE) was coated on carbon cloth to form the gas-diffusion layer. For comparison, a second MEA was prepared with Pt/MWNTs as the anode catalyst and Pt/MWNCs as the cathode catalyst following the similar procedure to that described above. The effective electrode area was 11.56 cm^2. A Pt loading of 0.25 and 0.5 mg cm^{-2} was maintained at the anode and the cathode, respectively. The MEAs were evaluated with a fuel cell test station by fixing it between two graphite plates which were had provision for gas flow (serpentine flow-through operation). The gas streams of pure hydrogen and oxygen were controlled by their respective mass flow controllers, and the flow rates were kept at 100 sccm, respectively. Hydrogen and oxygen were humidified using respective humidifiers before feeding into the anode and the cathode (anode and cathode humidifiers were maintained 10 and 5 °C above the cell temperature, respectively); in-line heating was provided to avoid condensation. The reactant gases were humidified with water to maintain the water content in the membrane electrolyte. The performance of fuel cell was studied at three different temperatures (40, 50 and 60 °C) under a back pressure of 2 bar.

3. Results and discussion

X-ray diffraction patterns of Pt/MWNCs and Pt/N-MWNCs are shown in Fig. 1. The patterns display the characteristic (1 1 1), (2 0 0), (2 2 0) and (3 1 1) reflections of face centered cubic crystalline Pt (JCPDS, No. 04-0802), together with the peak corresponding to hexagonal graphite. Raman spectra of MWNCs and N-MWNCs (Fig. 2) show the characteristic Stokes G peak at ~1580 cm^{-1} and D-band at ~1335 cm^{-1} for MWNCs. It can be seen from the Raman spectra that nitrogen doping leads to an up-shift in the bands. A shifting of 8 and 6 cm^{-1} can be seen in the characteristic D-band and G-band, respectively, and this indicates the appearance of a new type of disorder with nitrogen doping [24].

XPS has been employed to analyze further the samples. As shown in Fig. 3, the XPS spectrum exhibits distinct C1s, N1s and O1s peaks from N-MWNCs and an additional Pt4f peak from Pt/N-MWNCs. The amount of nitrogen incorporated in the N-MWNCs is about 4 at%. The peak centred around 400 eV corresponds to the N1s region, Fig. 4 shows the de-convoluted N1s region of N-MWNCs. The binding energy centred at 398.4 and 400.0 eV corresponds to 'pyridinic' and 'pyrrolic' nitrogen, respectively. The former refers to N atoms that contribute to the π system with one p electron, while the latter refers to N atoms with two p electrons in the π system, although not necessarily coordinated in a pentagonal arrangement as pyrrole [25], while that at 401.6 eV is commensurate with 'quaternary nitrogen' [22,26] which refers to N atoms that dope inside the graphitic carbon layers with a relatively higher binding energy. The coiled structure of MWNCs and N-MWNCs and the Pt nanoparticles dispersed over these supports can be seen in their respective SEM and TEM images (Fig. 5(a)–(d)).

Polarization plots were recorded with a d.c. load box. Prior to these studies, the electrodes were activated between open-circuit potential and high current densities, i.e., to activate the catalyst for oxygen reduction reaction [27]. Polarization plots taken at three different temperatures (40, 50 and 60 °C) with a cathode containing Pt/MWNCs and Pt/N-MWNCs, respectively, are presented in Fig. 6(a) and (b). The MEA constructed with Pt/N-MWNCs as the ORR catalyst has a maximum power density of 540 mW cm^{-2}, whereas the MEA with Pt/MWNCs has a maximum power density of 490 mW cm^{-2}. The improved performance with Pt/N-MWNCs as the ORR catalyst can be attributed to the formation of additional pentagons and heptagons and an increase in the reactivity of neighbouring carbon atoms because of nitrogen doping [28]. It

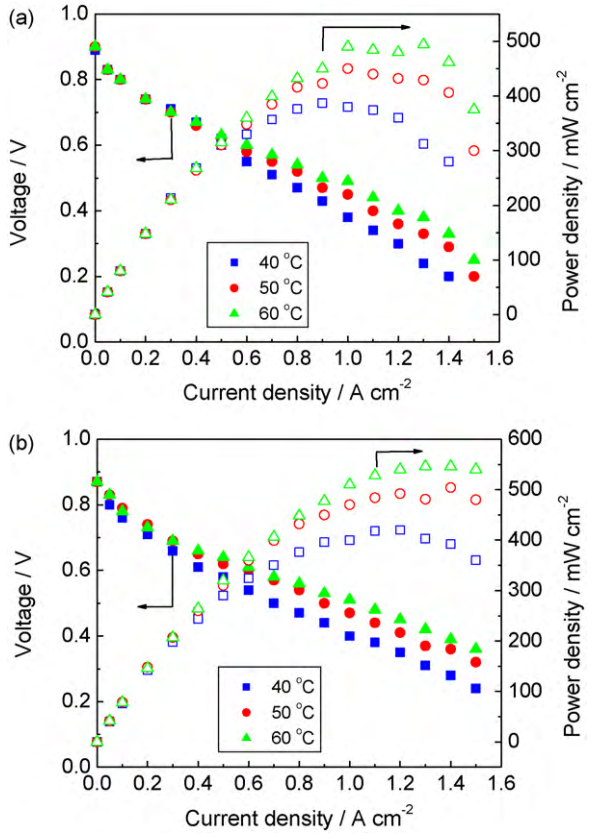

Fig. 6. Polarization graphs with (a) Pt/MWNCs and (b) Pt/N-MWNCs as cathode catalysts (Pt/MWNTs as anode for both (a) and (b)).

has been reported [28–30] that nitrogen doping introduces disorder in the MWNCs and the disordered structures and the defects can act as good anchoring sites for the deposition of Pt particles. N-doping of MWNCs increases the binding energy of the Pt atom to the substrate. In general, the more N atoms and the closer they are to the C atom which bonds directly to the Pt, the stronger is the binding energy [31]. The improved performance can also be attributed to the improved carbon-catalyst binding and increased electrical conductivity brought about by nitrogen doping. It has also been hypothesized that a synergistic support effect is found with N-MWNCs because the nitrogen-doped carbon nanostructures are known to decompose reactive intermediates such as hydrogen peroxide into oxygen formed during ORR [32]. Further studies are in progress for the use of N-MWNCs in direct alcohol fuel cells.

4. Conclusions

In summary, N-MWNCs prepared by plasma treatment of MWNCs has been demonstrated as catalyst support material for Pt nanoparticles for the ORR in PEMFCs. Full cells constructed with Pt/N-MWNCs and Pt/MWNCs as ORR catalyst show an improved performance of Pt/N-MWNCs catalyst compared with the Pt/MWNC catalyst. This has been attributed to the improved carbon-catalyst binding and increased electrical conductivity brought about by nitrogen doping. These results support the use of MWNCs or N-MWNCs as a new type of catalyst support material for PEMFC.

Acknowledgement

The authors thank AOARD (Asian Office of Aerospace Research & Development), USA and IITM (Indian Institute of Technology Madras), India for financial support.

References

[1] N. Punbusayakul, S. Talapatra, L. Ci, W. Surareungchai, P.M. Ajayan, Electrochem. Solid-State Lett. 10 (2007) F13.
[2] C. Soldano, S. Kar, S. Talapatra, S. Nayak, P.M. Ajayan, Nano Lett. 8 (2008) 4498.
[3] S. Talapatra, S. Kar, S.K. Pal, R. Vajtal, L. Ci, P. Victor, M.M. Shaijumon, S. Kaur, O. Nalamasu, P.M. Ajayan, Nat. Nanotechnol. 1 (2006) 112.
[4] P. Serp, M. Corrias, P. Kalck, Appl. Catal. A 253 (2003) 337.
[5] M. Terrones, Int. Mater. Rev. 49 (2004) 325.
[6] G.G. Wildgoose, C.E. Banks, R.G. Compton, Small 2 (2006) 182.
[7] T. Hayashida, L. Pan, J. Nakayama, Physica B 323 (2002) 352.
[8] M.M.J. Treacy, T.W. Ebbesen, J.M. Gibson, Nature 381 (1996) 678.
[9] X.Q. Chen, S.L. Zhang, D.A. Dikin, W.Q. Ding, R.S. Ruoff, L.J. Pan, Nano Lett. 3 (2003) 1299.
[10] M. Sevilla, G. Lota, A.B. Fuertes, J. Power Sources 171 (2007) 546.
[11] T. Hyeon, S. Han, Y. Sung, K. Park, Y. Kim, Angew. Chem. Int. Ed. 42 (2003) 4352.
[12] Y. Shao, G. Yin, Y. Gao, J. Power Sources 171 (2007) 558.
[13] B. Wang, J. Power Sources 152 (2005) 1.
[14] G. Wu, D. Li, C. Dai, D. Wang, Langmuir 24 (2008) 3566.
[15] X. Lepró, E. Terrés, Y. Vega-Cantú, F.J. Rodríguez-Macías, H. Muramatsu, Y.A. Kim, T. Hayahsi, M. Endo, M.R. Torres, M. Terrones, Chem. Phys. Lett. 463 (2008) 124.
[16] Y. Chen, J. Wang, H. Liu, R. Li, X. Sun, S. Ye, S. Knights, Electrochem. Commun. 11 (2009) 2071.
[17] R.A. Sidik, A.B. Anderson, N.P. Subramanian, S.P. Kumaraguru, B.N. Popov, J. Phys. Chem. B 110 (2006) 1787.
[18] C.L. Sun, L.C. Chen, M.C. Su, L.S. Hong, O. Chyan, C.Y. Hsu, K.H. Chen, T.F. Chang, L. Chang, Chem. Mater. 17 (2005) 3749.
[19] N. Li, Z. Wang, K. Zhao, Z. Shi, Z. Gu, S. Xu, Carbon 48 (2010) 255.
[20] L.S. Panchakarla, K.S. Subrahmanyam, S.K. Saha, A. Govindaraj, H.R. Krishnamurthy, U.V. Waghmare, C.N.R. Rao, Adv. Mater. 21 (2009) 4726.
[21] X. Li, H. Wang, J.T. Robinson, H. Sanchez, G. Diankov, H. Dai, J. Am. Chem. Soc. 131 (2009) 15939.
[22] R. Chetty, S. Kundu, W. Xia, M. Brona, W. Schuhmann, V. Chirila, W. Brandl, T. Reinecke, M. Muhler, Electrochim. Acta 54 (2009) 4208.
[23] A.L.M. Reddy, Synthesis of carbon nanotubes and their applications to fuel, cells and energy storage, May 2007, Dept. of Physics, Indian Institute of Technology Madras, Chennai, India, Ph.D Thesis, 104–112. http://www.cenlib.iitm.ac.in/docs/library/index.php?page=theses.
[24] L.G. Bulusheva, A.V. Okotrub, I.A. Kinloch, I.P. Asanov, A.G. Kurenya, A.G. Kudashov, X. Chen, H. Song, Phys. State Solidi B 245 (2008) 1971.
[25] J.R. Pels, F. Kapteijn, J.A. Moulijn, Q. Zhu, K.M. Thomas, Carbon 33 (1995) 1641.
[26] G. Wua, R. Swaidan, D. Li, N. Li, Electrochim. Acta 5 (2008) 7622.
[27] A.K. Shukla, M. Neergat, B. Parthasarathi, V. Jayaram, M.S. Hegde, J. Electroanal. Chem. 504 (2001) 111.
[28] C.H. Wang, H.Y. Du, Y.T. Tsai, C.P. Chen, C.J. Huang, L.C. Chen, K.H. Chen, H.C. Shih, J. Power Sources 171 (2007) 55.
[29] H. Sjöström, S. Stafström, M. Boman, J.E. Sundgren, Phys. Rev. Lett. 75 (1995) 1336.
[30] R.L. Jia, C.Y. Wang, S.M. Wang, J. Mater. Sci. 41 (2006) 6881.
[31] M.N. Groves, A.S.W. Chan, C. Malardier-Jugroot, M. Jugroot, Chem. Phys. Lett. 481 (2009) 214.
[32] S. Maldonado, K.J. Stevenson, J. Phys. Chem. B 109 (2005) 4707.
[33] M.M. Shaijumon, N. Rajalakshmi, S. Ramaprabhu, Appl. Phys. Lett. 88 (2006) 253105.